HHS Public Access

Author manuscript

Int J Obes (Lond). Author manuscript; available in PMC 2020 March 01.

Published in final edited form as:

Int J Obes (Lond). 2019 March ; 43(3): 475–486. doi:10.1038/s41366-018-0037-x.

CYP2A6 is associated with obesity: studies in human samples and a high fat diet mouse model

Kesheng Wang,
Department of Biostatistics and Epidemiology, College of Public Health, East Tennessee State University, Johnson City, TN, USA WANGK@mail.etsu.edu

Xue Chen,
Department of Health Sciences, College of Public Health, East Tennessee State University, Johnson City, TN, USA chenx1@etsu.edu

Stephen C. Ward,
Department of Pathology, Icahn School of Medicine at Mount Sinai, New York, NY 10029, USA Stephen.ward@mssm.edu

Ying Liu,
Department of Biostatistics and Epidemiology, College of Public Health, East Tennessee State University, Johnson City, TN, USA LIUY09@mail.etsu.edu

Youssoufou Ouedraogo,
Department of Biostatistics and Epidemiology, College of Public Health, East Tennessee State University, Johnson City, TN, USA OUEDRAOGO@mail.etsu.edu

Chun Xu,
Department of Health and Biomedical Sciences, College of Health Affairs, University of Texas Rio Grande Valley, Brownsville, TX 78520, USA chun.xu@utrgv.edu

Arthur I. Cederbaum, and
Department of Pharmacological Sciences, Icahn School of Medicine at Mount Sinai, New York, NY 10029, USA arthur.cederbaum@mssm.edu

Yongke Lu
Department of Health Sciences, College of Public Health, East Tennessee State University, Johnson City, TN, USA

Center of Excellence for Inflammation, Infectious Disease and Immunity, East Tennessee State University, Johnson City, TN, USA luy004@etsu.edu

Abstract

Background/Objectives—CYP2A6 (CYP2A5 in mice) is mainly expressed in the liver. Hepatic CYP2A6 expression is increased in patients with non-alcoholic fatty liver disease

Contact information: Yongke Lu, Department of Health Sciences, College of Public Health, East Tennessee State University, Lamb Hall, Johnson City, TN 37614-1700, USA; Tel.: +1 423 439 4575; Fax: 423-439-4562; luy004@etsu.edu.

CONFLICT OF INTEREST

The authors declare no conflict of interest.

(NAFLD). In mice, hepatic CYP2A5 is induced by high fat diet (HFD) feeding. Hepatic CYP2A5 is also increased in monosodium glutamate-induced obese mice. NAFLD is associated with obesity. In this study, we examined whether obesity is related to CYP2A6.

Subjects/Methods—Obesity genetic association study: The SAGE is a comprehensive genome-wide association study (GWAS) with case subjects having a lifetime history of alcohol dependence and control subjects never addicted to alcohol. We used 1030 control individuals with self-reported height and weight. A total of 12 single nucleotide polymorphisms (SNP) within the CYP2A6 gene were available. Obesity was determined as a BMI ≥ 30: 30–34.9 (Class I obesity) and ≥ 35 (Class II and III obesity). Animal experiment study: CYP2A5 knockout (*cyp2a5*$^{-/-}$) mice and wild type (*cyp2a5*$^{+/+}$) mice were fed HFD for 14 weeks. Body weight was measured weekly. After an overnight fast, the mice were sacrificed. Liver and blood were collected for biochemical assays.

Results—Single marker analysis showed that 3 SNPs (rs8192729, rs7256108, and rs7255443) were associated with class I obesity ($p<0.05$). The most significant SNP for obesity was rs8192729 (Odds Ratio=1.94, 95% Confidence intervals=1.21–3.10, p=0.00582). After HFD feeding, body weight was increased in *cyp2a5*$^{-/-}$ mice to a greater extent than in *cyp2a5*$^{+/+}$ mice, and fatty liver was more pronounced in *cyp2a5*$^{-/-}$ mice than in *cyp2a5*$^{+/+}$ mice. PPARα deficiency in *cyp2a5*$^{-/-}$ mice developed more severe fatty liver, but body weight was not increased significantly.

Conclusion—CYP2A6 is associated with human obesity; CYP2A5 protects against obesity and NAFLD in mice. PPARα contributes to the CYP2A5 protective effects on fatty liver but it opposes to the protective effects on obesity.

Keywords

FGF21; CYP2A5; PPARα; NAFLD

INTRODUCTION

Dysfunction in lipid metabolism and glucose homeostasis leads to obesity, which is related to diabetes, hepatic steatosis, hyperlipidemia, and insulin resistance. The liver plays an essential role in the control of glucose and lipid homeostasis. Cytochrome P450 (CYP) enzymes are a family of hemeprotein mainly expressed in liver. Some subfamilies of CYPs contribute to microsomal fatty acid oxidation. CYP4A was found to be contributive to non-alcoholic fatty liver in CYP2E1 knockout mice (ref. 1). CYP2E1 contributes to alcoholic fatty liver (ref. 2–3) and non-alcoholic fatty liver (ref. 4–5). Recently, CYP1B1 was reported to be a new modulator of liver lipid metabolism (ref. 6).

CYP2A is a subfamily of CYPs, which includes but does not limit to CYP2A6 in human and CYP2A5 in mice (ref. 7). Coumarin is 7-hydroxylated specifically by coumarin 7-hydroxylase encoded by the mouse cyp2a5 gene and human cyp2a6 gene (ref. 7). Thus, activity of coumarin 7-hydroxylase is accepted as a marker of CYP2A5/6 catalytic activity. In the rest of this article, CYP2A5 and CYP2A6 are generally referred to CYP2A, and in catalytic enzyme level, they are referred to coumarin 7-hydroxylase.

In the liver sections from patients with alcoholic liver diseases, CYP2A expression was detected to be increased (ref. 8). Consistently, in a mouse model, we found that expression

of CYP2A and activity of coumarin 7-hydroxylase were induced by alcohol feeding (ref. 9–10). However, alcoholic fatty liver was enhanced in cyp2a5 knockout (*cyp2a5*$^{-/-}$) mice, suggesting that CYP2A protects but does not contributes to alcoholic fatty liver (ref. 11–12). In the liver sections from patients with non-alcoholic fatty liver diseases, CYP2A expression was also detected to be increased (ref. 9). In an animal model, hepatic CYP2A protein was reported to be increased in monosodium glutamate-induced obese mice (ref. 13). But it is still unclear whether CYP2A protects against or contributes to obesity and non-alcoholic fatty liver.

Peroxisome proliferator-activated receptor α (PPARα) is a major to regulator for hepatic lipid metabolism. Interestingly, the basal level of PPARα was elevated in the *cyp2a5*$^{-/-}$ mice (ref. 11–12). Using Pparα and Cyp2a5 double knockout (P-A-) mice, we found that CYP2A cooperates with PPARα in mice to protect against alcoholic fatty liver (ref. 12). It is well known that PPARα regulates fatty acid oxidation and protects against non-alcoholic fatty liver (ref. 14–15). PPARα activation prevent obesity in ob/ob obese mice (ref. 16) and PPARα absence in *ob/ob* obese mice make the mice more obese (ref. 17), suggesting that PPARα may also protect against obesity. In this study we examined whether CYP2A interacts with PPARα to regulate obesity and non-alcoholic fatty liver.

MATERIALS AND METHODS

HUMAN SUBJECTS

The SAGE (Study of Addiction: Genetics and Environment) sample—The SAGE is a comprehensive genome-wide association study (GWAS) using approximately 4,000 unrelated subjects of European and African-American descent. It was funded as part of the Gene Environment Association Studies (GENEVA) initiative supported by the National Human Genome Research Institute (dbGaP study accession phs000092.v1.p1). Cases were 1,944 subjects with the primary phenotypes identified as having a lifetime history of alcohol dependence using DSM-IV criteria (ref. 18–19). Controls consisted of 1,965 subjects who had used alcohol, but had never been addicted to alcohol or other illicit substances. In the present study, we used 1030 Caucasian control individuals with self-reported height and weight. Those control individuals diagnosed as having drug dependence due to the likely genetic overlap between alcohol dependence and drug dependence were excluded. Participant characteristics are presented in Supplemental Table 1. There were more females than males in each weight class. The mean and ranges of age are similar in each weight class. Obesity was determined by body mass index (BMI), which was calculated by body weight (in kilograms) divided by squared height (in meters). Based on the magnitude of BMI (=kg/m^2), the individuals were classified into four categories: 18.5–24.9 (normal weight as controls), 25–29.9 (overweight), 30–34.9 (Class I obesity), and ≥ 35 (Class II and III obesity). Twelve individuals with BMI <18.5 were excluded in this study. Social factors used in this study were age and gender. Genotyping was performed by the Center for Inherited Disease Research using the Illumina Human1M-Duo BeadChip system. A total of 12 single nucleotide polymorphisms (SNPs) within the CYP2A6 and CYP2A7 genes were available in this sample (Table 1). All 12 SNPs were in Hardy-Weinberg equilibrium in the

controls (p>0.01). This study was approved by Internal Review Board (IRB) at East Tennessee State University (ETSU).

Statistical analyses—Hardy-Weinberg equilibrium was tested for all of the SNPs in individuals with normal weight as controls by using HAPLOVIEW software (ref. 20). Then, minor allele frequency (MAF) was determined for each SNP and the linkage disequilibrium (LD) structure was constructed using HAPLOVIEW software. Multiple logistic regression analysis of overweight, obesity I and obesity II+III, adjusted for age and sex, was performed using PLINK v1.07 (ref. 21). The asymptotic p-values for this test were observed while the odds ratio (OR) and its standard error were estimated. Haplotype analyses of obesity were performed for the SAGE sample using the PLINK software. Descriptive statistics for age and gender were conducted with SAS statistical software, version 9.4 (SAS Institute, Cary, NC, USA).

ANIMAL EXPERIMENTATION

Animals and Treatments—The colony of *cyp2a5*$^{-/-}$ mice was created by crossing male C57BL/6 *cyp2a5*$^{-/-}$ mice (ref. 22) (kindly provided by Dr. Xinxin Ding, SUNY College of Nanoscale Science and Engineering, Albany, NY, USA) and female C57BL/6 wild type mice (purchased from Charles River Laboratory, MA, USA). Littermates (*cyp2a5*$^{+/+}$) were bred as a colony of WT control. The *Ppara*$^{-/-}$ mice were purchased from Jackson Laboratory (Strain #008154). The colony of Pparα and Cyp2a5 double knockout mice (P-A- mice) was created by crossing the *Ppara*$^{-/-}$ mice with *Cyp2a5*$^{-/-}$ mice. Littermates not expressing Cyp2a5 but expressing Pparα (P+A-) and expressing Cyp2a5 but not expressing Pparα (P-A+) were used as control mice. All the mice were housed in temperature-controlled animal facilities with 12-hour light/12-hour dark cycles and were permitted consumption of tap water and Purina standard chow *ad libitum*. The mice received humane care, and experiments were carried out according to the criteria outlined in the Guide for the Care and Use of Laboratory Animals. The animal studies were approved by Animal Care and Use Committee at Icahn School of Medicine at Mount Sinai and University Committee on Animal Care at ETSU, respectively.

The female, 6–8 weeks mice (5 mice/group by randomization) were used to induce obesity and non-alcoholic fatty liver disease by feeding a high fat diet (HFD). The mice in control groups were fed control diet (CD). All mice were permitted consumption of tap water and HFD or CD *ad libitum*. Mouse body weight and diet consumption were measured weekly. In HFD, fat calories are 60%. HFD and CD contain the same amount (20.5%) of protein. The mice were fasted overnight (15 h) and then sacrificed. Blood was collected and serum levels of triglyceride, free fatty acids, β-hydroxyl butyrate, FGF21, insulin, adiponectin, leptin, and CTRP3 were measured using commercially available kits (supplemental Table 2). The livers were rapidly excised into fragments and washed with cold saline. Liver tissues from same lobes of different mice were put in neutral Formalin solution for paraffin bedding. The other liver tissue aliquots were stored at −80°C for future assays. Liver homogenates were prepared in ice-cold 0.15 M potassium chloride (KCL) and liver triglyceride content was measured using the same assay kit as serum triglyceride.

Glucose tolerance test, insulin tolerance test, and pyruvate tolerance test—For Glucose tolerance test and pyruvate tolerance test, the mice were subjected to an overnight fast (15h) followed by glucose or pyruvate injection ip at 1 g/kg and 2 g/kg, respectively. For insulin tolerance test, under feeding status the mice were injected with insulin ip at 2 U/kg. Blood was collected from tails for measuring blood glucose by Bayer Contour blood glucose meter.

Liver Histology—Liver sections with hematoxylin and eosin (H&E) staining were used for pathological evaluation as described before (ref. 2–3).

Liver microsomal CYP2E1 and CYP2A5 Activity—For liver microsomes preparation and microsomal CYP2E1 and CYP2A5 (coumarin 7-hydroxylase) activity assays please see reference (ref. 9–12).

Western Blotting—The SDS-PAGE and chemiluminescence imaging was carried out as described before (ref. 9–12). β-actin was detected as a protein loading control. Anti-CYP2E1 and anti-CYP2A antibodies were gifts from Dr. Jerome Lasker (Hackensack Biomedical Research Institute, Hackensack, NJ, USA) and Dr. Risto Juvonen (Department of Pharmacology and Toxicology, University of Kuopio, Kuopio, Finland), respectively. Anti-ADRP was from Abcam (Cambridge, MA, USA).

RESULTS

Genetic association study: CYP2A6 gene is associated with obesity

Single marker analysis showed that 3 SNPs (rs8192729, rs7256108, and rs7255443) in the CYP2A6 gene were associated with class I obesity ($p<0.05$) (Table 1). The most significant SNP for obesity was rs8192729 (OR=1.94, 95%CI=1.21–3.10, $p=5.82\times10^{-3}$). The SNP rs7251418 revealed a borderline association with class II and III obesity (OR=1.34, 95%CI=0.96–1.87, p=0.0878). The pairwise LD statistics (r^2) for 10 SNPs were assessed for controls with normal weight using HAPLOVIEW (Supplemental Figure 1). Rough rule of thumb, values of r^2 >1/3 might indicate sufficiently strong LD to be used for fine mapping (ref. 23). Table 2 shows eight haplotypes associated with class I obesity. The A-G haplotype from rs8192729-rs7256108 (r^2 = 0.94 between the two SNPs) and the A-T haplotype from rs8192729-rs7255443 (r^2 = 0.94 between the two SNPs) showed the most significant associations with class I obesity ($p = 5.82\times10^{-3}$). These results suggest that CYP2A6 gene is associated with obesity in human, especially class I obesity.

After HFD feeding, c*yp2a5*$^{-/-}$ mice exhibit more body weight gain than c*yp2a5*$^{+/+}$ mice

The female c*yp2a5*$^{-/-}$ and c*yp2a5*$^{+/+}$ mice were fed HFD or CD for 3 months. After HFD feeding, the c*yp2a5*$^{-/-}$ mice exhibited a significant increase in body weight starting from the 6th week, while the significant increase in body weight was observed in c*yp2a5*$^{+/+}$ mice starting from the 9th week. The body weight was increased in HFD-fed c*yp2a5*$^{-/-}$ mice to a greater extent than in HFD-fed c*yp2a5*$^{+/+}$ mice starting from the 6th week (Fig 1 A). After HFD feeding, serum triglyceride was increased by 2-fold in c*yp2a5*$^{-/-}$ mice, but it was increased only 20% in c*yp2a5*$^{+/+}$ mice (Fig 1 B). Similarly, serum glucose was not

significantly increased in c*yp2a5*$^{+/+}$ mice but it was increased about 2.5-fold in c*yp2a5*$^{-/-}$ mice (Fig 1 C). In response to glucose challenge, the HFD-fed c*yp2a5*$^{-/-}$ mice exhibited a more severe glucose intolerance than the HFD-fed c*yp2a5*$^{+/+}$ mice did (Fig 1 D). However, after 30min of insulin injection, there was no significant difference in blood glucose reduction between the c*yp2a5*$^{-/-}$ mice and c*yp2a5*$^{+/+}$ mice, either HFD-fed or CD-fed (Fig 1 E). After 2 h of insulin injection, while blood glucose remained reduced in CD-fed c*yp2a5*$^{-/-}$ mice, it started to recover in other three groups (Fig 1 E). Generally, CYP2A protects against HFD-induced dysfunction in lipid metabolism and glucose homeostasis, and HFD-induced obesity is protected by CYP2A.

HFD-induced fatty liver is more pronounced in c*yp2a5*$^{-/-}$ mice than in c*yp2a5*$^{+/+}$ mice

After HFD feeding, liver contents of triglyceride were increased in c*yp2a5*$^{-/-}$ mice to a greater extent than in c*yp2a5*$^{+/+}$ mice (Fig 2 A). Consistently, HFD-induced fatty liver as indicated by lipid droplets in H&E stained liver sections was more pronounced in c*yp2a5*$^{-/-}$ mice than in c*yp2a5*$^{+/+}$ mice (Fig 2B, 2C). Expression of adipose differentiation-related protein (ADRP), a marker of fatty liver (ref. 24), was increased in c*yp2a5*$^{-/-}$ mice more than in c*yp2a5*$^{+/+}$ mice (Fig 2 D). Fibroblast growth factor 21 (FGF21) is mainly expressed in liver and released into blood (ref. 25). Basal levels of serum FGF21 were elevated in *cyp2a5*$^{-/-}$ mice. HFD induced FGF21 in *cyp2a5*$^{+/+}$ mice but did not induce FGF21 in *cyp2a5*$^{-/-}$ mice (Fig 2F). As expected, there was no hepatic CYP2A expression in c*yp2a5*$^{-/-}$ mice (Fig 2 D), activity of coumarin 7-hydroxylase was almost undetectable in hepatic microsomes isolated from c*yp2a5*$^{-/-}$ mice (Fig 2 E). Even though hepatic activity coumarin 7-hydroxylase and expression of CYP2A were detectable in c*yp2a5*$^{+/+}$ mice, they were not induced by HFD feeding (Fig 2D, 2E). CYP2E1, both activity and protein expression, was comparable in c*yp2a5*$^{-/-}$ mice and c*yp2a5*$^{+/+}$ mice, and they were induced by HFD feeding in both c*yp2a5*$^{-/-}$ mice and c*yp2a5*$^{+/+}$ mice (Fig 2D, 2E). These results suggest that HFD-induced fatty liver is more pronounced in c*yp2a5*$^{-/-}$ mice than in c*yp2a5*$^{+/+}$ mice, which is not related to CYP2E1.

PPARα absence in c*yp2a5*$^{-/-}$ mice blunts HFD-induced obesity but enhances HFD-induced fatty liver

Female PPARα and CYP2A5 double knockout mice (P-A- mice), their female littermates not expressing CYP2A5 but expressing PPARα (P+A-) or expressing CYP2A5 but not expressing PPARα (P-A+), were fed HFD or CD for 10 weeks. While P+A- mice (equivalent to cyp2a5$^{-/-}$ mice) developed severe obesity (Fig. 3A **middle panel**), surprisingly, body weight in P-A- mice (Fig. 3A **left panel**) and P-A+ mice (equivalent to *Pparα*$^{-/-}$ mice) (Fig. 3A **right panel**) was not significantly increased in response to HFD feeding. Adipose tissue section H&E staining showed that sizes of adipocyte in P+A- mice were larger than those in P-A- mice and P-A+ mice (Fig. 3B). Although there was no difference in serum insulin levels among P-A- mice, P+A-mice and P-A+ mice (Supplemental Fig. 2A), P+A- mice exhibited more severe glucose intolerance (Fig. 3C **middle panel**) than P-A- mice (Fig. 3C **left panel**) and P-A+ mice (Fig. 3C **right panel**); HFD feeding worsen the glucose intolerance in P+A- mice but HFD had no effect on glucose intolerance in P-A- mice and P-A+ mice (Fig. 3C). Pyruvate tolerance test showed that blood glucose in response to pyruvate injection was lower in P-A- mice than in P+A-

mice (Fig. 3D), suggesting a lower capacity for liver gluconeogenesis in P-A- mice than in P +A- mice.

Using Bio-Plex mouse diabetes panel kit we screened 8 diabetes-related cytokines and found that serum leptin was induced by HFD in P+A- mice but not in P-A- mice and P-A+ mice (Fig. 3E). In contrast, serum ghrelin was induced in P-A- mice and P-A+ mice but not in P +A- mice (Fig. 3E). The other 6 cytokines including insulin, glucagon, PAI-1, resistin, GIP, and GLP-1 had no or little changes (Supplemental Fig. 5).

While HFD-induced obesity was suppressed in P-A- mice, HFD-induced fatty liver was more pronounced in P-A- mice than in P+A- mice and P-A+ mice, even CD-fed P-A- mice exhibited a weak steatosis but CD-fed P+A- mice or P-A+ mice did not (Fig. 4A). Immunohistochemistry staining indicates that most lipid droplets were surrounded by ADRP (Supplemental Fig. 3). Sirius Red staining showed that HFD-induced collagen fiber was mainly located in sinusoids (Supplemental Fig. 4). There were no significant differences in serum levels of triglyceride and aspartate transaminase (ALT) between P-A- mice and P+A- mice (Supplemental Fig. 2B, 2C). Although serum glycerol, a marker of adipolysis, had no significant difference among the groups (Supplemental Fig. 2D), serum free fatty acids, which are mainly derived from adipose tissue after an overnight fasting, was lower in P+A- mice than in P-A- mice and P-A+ mice (Fig. 4B),. Serum β-hydroxylbutyrate, indicative of ketogenesis, was lower in P-A- mice and P-A+ mice than in P+A- mice (Fig. 4C).

FGF21 is regulated by PPARα (ref. 25). Serum FGF21 was higher in P+A- mice than in P-A- and P-A+ mice (Fig. 4D). FGF21 may exert its effect via adiponectin (ref. 26–27). However, we did not see any significant difference in serum adiponectin between P-A- and P +A- mice (Fig. 4E). Instead, basal levels of serum C1q TNF Related Protein 3 (CTRP3), a new adipokine (ref.28), were upregulated in P-/A- mice and P-/A+ mice, and HFD feeding suppressed CTRP3 in P-/A- mice and P-/A+ mice but not in P+/A- mice, suggesting that PPARα contributes to maintaining the serum levels of CTRP3 stable in P+A- mice (Fig. 4F).

DISCUSSION

Kirby et al first reported that hepatic CYP2A may regulate lipid metabolism (ref.29). Recently it was found that fatty acids can induce CYP2A in hepatocytes (ref.30–31). Previously, we found that CYP2A protects against alcoholic fatty liver (ref.11–12). In this study, we identified an association of CYP2A6 gene with obesity in human subjects. In animal experiments, we found that obesity and hepatic steatosis was more severe in *cyp2a5*$^{-/-}$ mice than in c*yp2a5*$^{+/+}$ mice, suggesting that CYP2A protects against obesity and non-alcoholic fatty liver.

It is well known that PPARα can regulate liver fatty acid oxidation and prevent fatty liver. Fasted *pparα*$^{-/-}$ mice exhibited more severe steatosis than fasted wild type mice (ref.14–15). Global or liver-specific PPARα absence revealed an enhanced fatty liver in response to methionine and choline deficient diet (ref.32). Consistently, P-A- mice developed more severe fatty liver than P+A- mice did, and serum free fatty acids was higher in P-/A- mice and P-A+ mice than in P+/A- mice, suggesting that PPARα may synergize with CYP2A to

protect against hepatic steatosis i.e. the protective effects of CYP2A on non-alcoholic fatty liver are augmented but not masked by PPARα. PPARα can also regulate glucose homeostasis (ref.33). Gluconeogenesis indicated by pyruvate tolerance test and glucose intolerance indicated by glucose tolerance test were lower in P-/A- and P-/A+ mice than in P +A- mice, suggesting that PPARα regulates gluconeogenesis and glucose homeostasis independent of CYP2A. More severe glucose and pyruvate intolerance in P+/A- mice than in P-/A- mice suggests that CYP2A regulates glucose homeostasis via PPARα. Both P-/A- mice and P-/A+ mice exhibited comparable higher serum free fatty acids, lower serum β-hydroxylbutyrate, and lower serum glucose (glucose tolerance and gluconeogenesis), but only P-/A- mice revealed a more pronounced fatty liver, suggesting that PPARα-regulated lipid metabolism and gluconeogenesis are prime factors for the development of severe fatty liver in P-/A- mice, and CYP2A deficiency can enhance the PPARα deficiency-related steatosis. PPARα was upregulated in *cyp2a5*$^{-/-}$ mice (ref.11–12). Thus, elevation of PPARα in *cyp2a5*$^{-/-}$ mice might be a compensatory response to improve the impaired metabolism capacity caused by the deletion of CYP2A. Further deletion of PPARα in *cyp2a5*$^{-/-}$ mice causes de-compensation and induces severe fatty liver.

Recently it was found that failure to increase PPARα-regulated free fatty acid oxidation may be more prone to developing obesity because PPARα deficiency in *ob/ob* obese mice makes the mice become more obese (ref.17). Fat is mainly stored in adipose tissue in the form of triglyceride. When the fat in adipose tissue is saturated, the fat “overflows” from adipose tissue to liver, which contributes to hepatic steatosis (ref.34). Indeed, liver fat is mainly from adipose tissue (ref.35). In this study, while fatty liver was more severe in P-/A- mice than in P+/A- mice, body weight gain (obesity) was less in P-/A- mice than in P+/A- mice. When fat is subjected to lipolysis in adipose tissue, free fatty acids will be released into blood, so fat flow from adipose tissue to liver is in the form of serum free fatty acids. Compared with P+A- mice, P-/A- mice exhibited higher serum free fatty acids, suggesting a stronger adipose lipolysis, which may cause less obese and more severe fatty liver. Therefore, this observation is still in agreement with the notion that “fat flow” from adipose to liver contributes to hepatic steatosis. On the other hand, both P-/A- mice and P-/A+ mice exhibited identical less obesity and higher serum free fatty acids, but only P-/A- mice developed severe fatty liver, suggesting that CYP2A5 deficiency is essential for the severe fatty liver development. Thus, the interaction between CYP2A and PPARα has opposing effects: protecting against fatty liver but promoting obesity.

FGF21 is a modulator of lipid metabolism and glucose homeostasis (ref.36). FGF21 attenuates hyperglycemia by increasing energy metabolism in adipose tissues (ref.37); hepatic FGF21 transgenic mice were protected from diet-induced obesity (ref.25). Treatment with FGF21 also acts directly on the liver to modulate hepatic metabolism (ref.37) and FGF21 knockdown caused both hepatic steatosis and hypertriglyceridemia (ref.38). We found that recombinant FGF21 (rFGF21) treatment blunted hypertriglyceridemia induced by alcohol feeding in *ppara*$^{-/-}$ mice (ref.12), so PPARα regulates lipid metabolism through FGF21. FGF21 is mainly produced in liver and is released from liver into blood. FGF21 can target adipocytes because FGF21 exerts its effect via binding to FGF receptor 1 which is mainly expressed in adipocytes (ref.37 and 39). Thus, interaction between adipose tissue and liver might be mediated by the liver-released FGF21. Because FGF21 is regulated by

PPARα (ref.38, ref.40–41), serum FGF21 was much lower in P-/A- mice and P-/A+ mice than in P+/A- mice (Fig.4D). Free fatty acids are endogenous ligands to activate PPARα, but serum free fatty acids from adipose tissue do not activate PPARα, instead, it is *de novo* synthesized fatty acids that activate PPARα (ref.42). Fatty acid synthase (FAS) is elevated in *cyp2a5*$^{-/-}$ mice (ref.11). Thus, in *cyp2a5*$^{-/-}$ mice fatty acids *de novo* synthesized by FAS may activate the already elevated PPARα. Therefore, serum FGF21 were still higher in P+A- mice than in P-/A- mice and P-/A+ mice even though serum free fatty acids (mainly derived from adipose lipolysis) were lower in P+/A- mice than in P-/A- mice and P-/A+ mice. FGF21 may exert effect via adiponectin (ref.26–27). However, no difference in serum adiponectin between P-A- and P+A- mice was observed. Instead, serum leptin was dramatically induced by HFD in P+/A- mice but not in P-/A- mice and P-/A+ mice, which is similar to changes of serum FGF21. In fact, leptin is a potential regulator of FGF21 (ref.43) and FGF21 can promote metabolic homeostasis via leptin (ref.44). In addition, another adipokine CTRP3 also protected against hepatic steatosis (ref.45). It is possible that PPARα regulates interaction between liver and adipose tissue through the liver released FGF21 and adipose tissue released adipokines. Whether CYP2A protects against obesity and fatty liver via interacting with a PPARα-FGF21-adipokine axis needs further studies.

In this study, we evaluated glucose homeostasis during HFD feeding in a few colonies of mice. The P+/A- and P-A- mice are new colonies created in our lab; HFD can deteriorate glucose intolerance in P+A- mice but not in P-A- mice. For observing an effect of HFD on glucose intolerance, the optimal fasting time was 6 h because the longer fasting times (18 or 24 h) diminished the HFD-enhancing effect on glucose intolerance (ref 46). In this study, the mice were fasted for 15 h before glucose tolerance test, and the HFD-enhancing effect on glucose intolerance was still observed in P+A- mice but not in P-A- mice. If a 6 h of fasting make the P-A- mice exhibit a HFD-enhancing effect, probably this HFD-enhancing effect in P-A- mice is still less than in P-A+ mice. The P-A+ mice are equivalent to *ppara*$^{-/-}$mice and our observation with glucose homeostasis in P-A+ mice is consistent with others' reports (ref. 14, 15). The *cyp2a5*$^{-/-}$ mice exhibited obvious glucose intolerance, which is consistent with our previous report that alcohol can induce hyperglycemia in *cyp2a5*$^{-/-}$ mice but not in c*yp2a5*$^{+/+}$ mice (ref.11). However, we did not observe a blood glucose recovering in *cyp2a5*$^{-/-}$ mice within 2 h after an insulin injection. FGF21 can augment insulin activity to promote glucose uptake in adipocytes (ref. 36). Basal levels of serum FGF21 was higher in *cyp2a5*$^{-/-}$ mice than in c*yp2a5*$^{+/+}$ mice. It needs further studies to address whether elevated FGF21 in *cyp2a5*$^{-/-}$ mice contributes to sustained reduction of blood glucose in response to insulin injection.

In summary, genetic association study suggests that CYP2A6 gene is associated with obesity in human subjects. Animal experiments suggest that CYP2A protects against obesity and nonalcoholic fatty liver in mice, and through regulating lipid metabolism and glucose homeostasis, PPARα contributes to the CYP2A protective effects on fatty liver but it opposes to the CYP2A protective effects on obesity.

Supplementary Material

Refer to Web version on PubMed Central for supplementary material.

Acknowledgments

Funding support for the SAGE was provided through the NIH Genes, Environment and Health Initiative (GEI) Grant U01 HG004422. SAGE is one of the GWAS funded as part of the GENEVA under GEI. Assistance with phenotype harmonization and genotype cleaning, as well as with general study coordination, was provided by the GENEVA Coordinating Center (Grant U01 HG004446). Assistance with data cleaning was provided by the National Center for Biotechnology Information. Support for collection of datasets and samples were provided by COGA (Grant U10 AA008401), COGEND (Grant P01 CA089392), and FSCD (Grant R01 DA013423). Funding support for genotyping, which was performed at the Johns Hopkins University Center for Inherited Disease Research, was provided by NIH GEI Grant U01HG004438, NIAAA, NIDA, and the NIH contract "High throughput genotyping for studying the genetic contributions to human disease" (HHSN268200782096C). The datasets used for the analyses described in this manuscript were obtained from dbGaP at http://www.ncbi.nlm.nih.gov/projects/gap/cgibin/study.cgi study_id=phs000092.v1.p1 through dbGaP accession number phs000092.v1.p.1.

We thank Dr. Xinxin Ding for the *cyp2a5*$^{-/-}$ mice, Dr. Jerome Lasker for anti-CYP2E1 IgG and Dr. Risto Juvonen for anti-CYP2A5 IgG. This study is partially supported by USPHS grants AA-024723.

List of Abbreviations

ADRP	adipose differentiation-related protein
ALT	aspartate transaminase
BMI	body mass index
CD	control diet
CTRP3	C1q TNF Related Protein 3
CYP2A6	cytochrome P450 2A6
FAS	Fatty acid synthase
FGF21	fibroblast growth factor 21
GENEVA	gene Environment Association Studies
GWAS	genome-wide association study
HFD	high fat diet
LD	linkage disequilibrium
MAF	minor allele frequency
OR	odds ratio
PPARα	peroxisome proliferator-activated receptor α
SNP	single nucleotide polymorphism.

References

1. Leclercq IA, Farrell GC, Field J, Bell DR, Gonzalez FJ, Robertson GR. CYP2E1 and CYP4A as microsomal catalysts of lipid peroxides in murine nonalcoholic steatohepatitis. J Clin Invest. 2000; 105:1067–75. [PubMed: 10772651]

2. Lu Y, Zhuge J, Wang X, Bai J, Cederbaum AI. Cytochrome P450 2E1 contributes to ethanol-induced fatty liver in mice. Hepatology. 2008; 47:1483–94. [PubMed: 18393316]
3. Lu Y, Wu D, Wang X, Ward SC, Cederbaum AI. Chronic alcohol-induced liver injury and oxidant stress are decreased in cytochrome P4502E1 knockout mice and restored in humanized cytochrome P4502E1 knock-in mice. Free Radic Biol Med. 2010; 49:1406–16. [PubMed: 20692331]
4. Abdelmegeed MA, Banerjee A, Yoo SH, Jang S, Gonzalez FJ, Song BJ. Critical role of cytochrome P450 2E1 (CYP2E1) in the development of high fat-induced non-alcoholic steatohepatitis. J Hepatol. 2012; 57:860–6. [PubMed: 22668639]
5. Zong H, Armoni M, Harel C, Karnieli E, Pessin JE. Cytochrome P-450 CYP2E1 knockout mice are protected against high-fat diet-inducedobesity and insulin resistance. Am J Physiol Endocrinol Metab. 2012; 302:E532–9. [PubMed: 22185839]
6. Larsen MC, Bushkofsky JR, Gorman T, Adhami V, Mukhtar H, Wang S, et al. Cytochrome P450 1B1: An unexpected modulator of liver fatty acid homeostasis. Arch Biochem Biophys. 2015; 571:21–39. [PubMed: 25703193]
7. Su T, Ding X. Regulation of the cytochrome P450 2A genes. Toxicol Appl Pharmacol. 2004; 199:285–94. [PubMed: 15364544]
8. Niemelä O, Parkkila S, Juvonen RO, Viitala K, Gelboin HV, Pasanen M. Cytochromes P450 2A6, 2E1, and 3A and production of protein-aldehyde adducts in the liver of patients with alcoholic and non-alcoholic liver diseases. J Hepatol. 2000; 33:893–901. [PubMed: 11131450]
9. Lu Y, Zhuge J, Wu D, Cederbaum AI. 2011; Ethanol induction of CYP2A5: permissive role for CYP2E1. Drug Metab Dispos. 39:330–6. [PubMed: 21051534]
10. Lu Y, Zhang XH, Cederbaum AI. Ethanol induction of CYP2A5: role of CYP2E1-ROS-Nrf2 pathway. Toxicol Sci. 2012; 128:427–38. [PubMed: 22552773]
11. Hong F, Liu X, Ward SS, Xiong H, Cederbaum AI, Lu Y. Absence of cytochrome P450 2A5 enhances alcohol-induced liver injury in mice. Dig Liver Dis. 2015; 47:470–477. [PubMed: 25804444]
12. Chen X, Ward SC, Cederbaum AI, Xiong H, Lu Y. Alcoholic fatty liver is enhanced in CYP2A5 knockout mice: The role of the PPARα-FGF21 axis. Toxicology. 2017; 379:12–21. [PubMed: 28131861]
13. Tomankova V, Liskova B, Skalova L, Bartikova H, Bousova I, Jourova L, et al. Altered cytochrome P450 activities and expression levels in the liver and intestines of the monosodium glutamate-induced mouse model of human obesity. Life Sci. 2015; 133:15–20. [PubMed: 25998026]
14. Kersten S, Seydoux J, Peters JM, Gonzalez FJ, Desvergne B, Wahli W. Peroxisome proliferator-activated receptor alpha mediates the adaptive response to fasting. J Clin Invest. 1999; 103:1489–98. [PubMed: 10359558]
15. Leone TC, Weinheimer CJ, Kelly DP. A critical role for the peroxisome proliferator-activated receptor alpha (PPARalpha) in the cellular fasting response: the PPARalpha-null mouse as a model of fatty acid oxidation disorders. Proc. Natl. Acad. Sci. USA. 1999; 96:7473–7478. [PubMed: 10377439]
16. Huang J, Jia Y, Fu T, Viswakarma N, Bai L, Rao MS, et al. Sustained activation of PPARα by endogenous ligands increases hepatic fatty acid oxidation and prevents obesity in ob/ob mice. FASEB J. 2012; 26:628–38. [PubMed: 22009939]
17. Gao Q, Jia Y, Yang G, Zhang X, Boddu PC, Petersen B, et al. PPARα-Deficient ob/ob Obese Mice Become More Obese and Manifest Severe Hepatic Steatosis Due to Decreased Fatty Acid Oxidation. Am J Pathol. 2015; 185:1396–408. [PubMed: 25773177]
18. Bierut LJ, Agrawal A, Bucholz KK, Doheny KF, Laurie C, Pugh E, et al. A genome-wide association study of alcohol dependence. Proc Natl Acad Sci U S A. 2010; 107:5082–87. [PubMed: 20202923]
19. Wang KS, Liu X, Zhang QY, Pan Y, Aragam N, Zeng M. Meta-analysis of two genome-wide association studies identifies 3 new loci for alcohol dependence. J Psychiatr Res. 2011; 45:1419–1425. [PubMed: 21703634]
20. Barrett JC, Fry B, Maller J, Daly MJ. Haploview: analysis and visualization of LD and haplotype maps. Bioinformatics. 2005; 21:263–5. [PubMed: 15297300]

21. Purcell S, Neale B, Todd-Brown K, Thomas L, Ferreira MA, Bender D, et al. PLINK: a tool set for whole-genome association and population-based linkage analyses. Am J Hum Genet. 2007; 81:559–575. [PubMed: 17701901]
22. Zhou X, Zhuo X, Xie F, Kluetzman K, Humphreys WG, Ding X. Role of CYP2A5 in the clearance of nicotine and cotinine: insights from studies on a Cyp2a5-null mouse model. J Pharmacol Exp Ther. 2010; 332:578–87. [PubMed: 19923441]
23. Ardlie KG, Kruglyak L, Seielstad M. Patterns of linkage disequilibrium in the human genome. Nat Rev Genet. 2002; 3:299–309. [PubMed: 11967554]
24. Motomura W, Inoue M, Ohtake T, Takahashi N, Nagamine M, Tanno S, et al. Up-regulation of ADRP in fatty liver in human and liver steatosis in mice fed with high fat diet. Biochem Biophys Res Commun. 2006; 340:1111–8. [PubMed: 16403437]
25. Luo Y, McKeehan WL. Stressed Liver and Muscle Call on Adipocytes with FGF21. Front Endocrinol (Lausanne). 2013; 4:194. [PubMed: 24385972]
26. Holland WL, Adams AC, Brozinick JT, Bui HH, Miyauchi Y, Kusminski CM, et al. An FGF21-adiponectin-ceramide axis controls energy expenditure and insulin action in mice. Cell Metab. 2013; 17:790–7. [PubMed: 23663742]
27. Lin Z, Tian H, Lam KS, Lin S, Hoo RC, Konishi M, Itoh, et al. Adiponectin mediates the metabolic effects of FGF21 on glucose homeostasis and insulin sensitivity in mice. Cell Metab. 2013; 17:779–89. [PubMed: 23663741]
28. Li Y, Wright GL, Peterson JM. C1q/TNF-Related Protein 3 (CTRP3) Function and Regulation. Compr Physiol. 2017; 7:863–878. [PubMed: 28640446]
29. Kirby GM, Nichols KD, Antenos M. CYP2A5 induction and hepatocellular stress: an adaptive response to perturbations of heme homeostasis. Curr Drug Metab. 2011; 12:186–97. [PubMed: 21395539]
30. Cui Y, Wang Q, Yi X, Zhang X. Effects of Fatty Acids on CYP2A5 and Nrf2 Expression in Mouse Primary Hepatocytes. Biochem Genet. 2016; 54:29–40. [PubMed: 26423681]
31. Wang XH, Cui XX, Sun XQ, Wang XH, Li XC, Qi Y, et al. High Fat Diet-Induced Hepatic 18-Carbon Fatty Acids Accumulation Up-Regulates CYP2A5/CYP2A6 via NF-E2-Related Factor 2. Front Pharmacol. 2017; 8:233. [PubMed: 28555106]
32. Montagner A, Polizzi A, Fouché E, Ducheix S, Lippi Y, Lasserre F, et al. Liver PPARα is crucial for whole-body fatty acid homeostasis and is protective against NAFLD. Gut. 2016; 65:1202–14. [PubMed: 26838599]
33. Peeters A, Baes M. 2010Role of PPARα in hepatic carbohydrate metabolism. PPAR Res.
34. Gurevich-Panigrahi T, Panigrahi S, Wiechec E, Los M. Obesity: pathophysiology and clinical management. Curr Med Chem. 2009; 16:506–21. [PubMed: 19199918]
35. Donnelly KL, Smith CI, Schwarzenberg SJ, Jessurun J, Boldt MD, Parks EJ. Sources of fatty acids stored in liver and secreted via lipoproteins in patients with nonalcoholic fatty liver disease. J Clin Invest. 2005; 115:1343–51. [PubMed: 15864352]
36. Kharitonenkov A, Shiyanova TL, Koester A, Ford AM, Micanovic R, Galbreath EJ, et al. FGF-21 as a novel metabolic regulator. J Clin Invest. 2005; 115:1627–35. [PubMed: 15902306]
37. Fisher FM, Estall JL, Adams AC, Antonellis PJ, Bina HA, Flier JS, Kharitonenkov A, et al. Integrated regulation of hepatic metabolism by fibroblast growth factor 21 (FGF21) in vivo. Endocrinology. 2011; 52:2996–3004.
38. Badman MK, Pissios P, Kennedy AR, Koukos G, Flier JS, Maratos-Flier E. Hepatic fibroblast growth factor 21 is regulated by PPARalpha and is a key mediator of hepatic lipid metabolism in ketotic states. Cell Metab. 2007; 5:426–437. [PubMed: 17550778]
39. Potthoff MJ, Kliewer SA, Mangelsdorf DJ. Endocrine fibroblast growth factors 15/19 and 21: from feast to famine. Genes Dev. 2012; 26:312–24. [PubMed: 22302876]
40. Inagaki T, Dutchak P, Zhao G, Ding X, Gautron L, Parameswara V, et al. Endocrine regulation of the fasting response by PPARalpha-mediated induction of fibroblast growth factor 21. Cell Metab. 2007; 5:415–25. [PubMed: 17550777]
41. Lundåsen T, Hunt MC, Nilsson LM, Sanyal S, Angelin B, Alexson SE, et al. PPARalpha is a key regulator of hepatic FGF21. Biochem Biophys Res Commun. 2007; 360:437–440. [PubMed: 17601491]

42. Chakravarthy MV, Pan Z, Zhu Y, Tordjman K, Schneider JG, Coleman T, et al. "New" hepatic fat activates PPARalpha to maintain glucose, lipid, and cholesterol homeostasis. Cell Metab. 2005; 1:309–22. [PubMed: 16054078]

43. Asrih M, Veyrat-Durebex C, Poher AL, Lyautey J, Rohner-Jeanrenaud F, Jornayvaz FR. Leptin as a Potential Regulator of FGF21. Cell Physiol Biochem. 2016; 38:1218–25. [PubMed: 26982498]

44. Véniant MM, Hale C, Helmering J, Chen MM, Stanislaus S, Busby J, et al. FGF21 promotes metabolic homeostasis via white adipose and leptin in mice. PLoS One. 2012; 7:e40164. [PubMed: 22792234]

45. Peterson JM, Seldin MM, Wei Z, Aja S, Wong GW. CTRP3 attenuates diet-induced hepatic steatosis by regulating triglyceride metabolism. Am J Physiol Gastrointest Liver Physiol. 2013; 305:G214–24. [PubMed: 23744740]

46. Andrikopoulos S, Blair AR, Deluca N, Fam BC, Proietto J. Evaluating the glucose tolerance test in mice. Am J Physiol Endocrinol Metab. 2008; 295:E1323–32. [PubMed: 18812462]

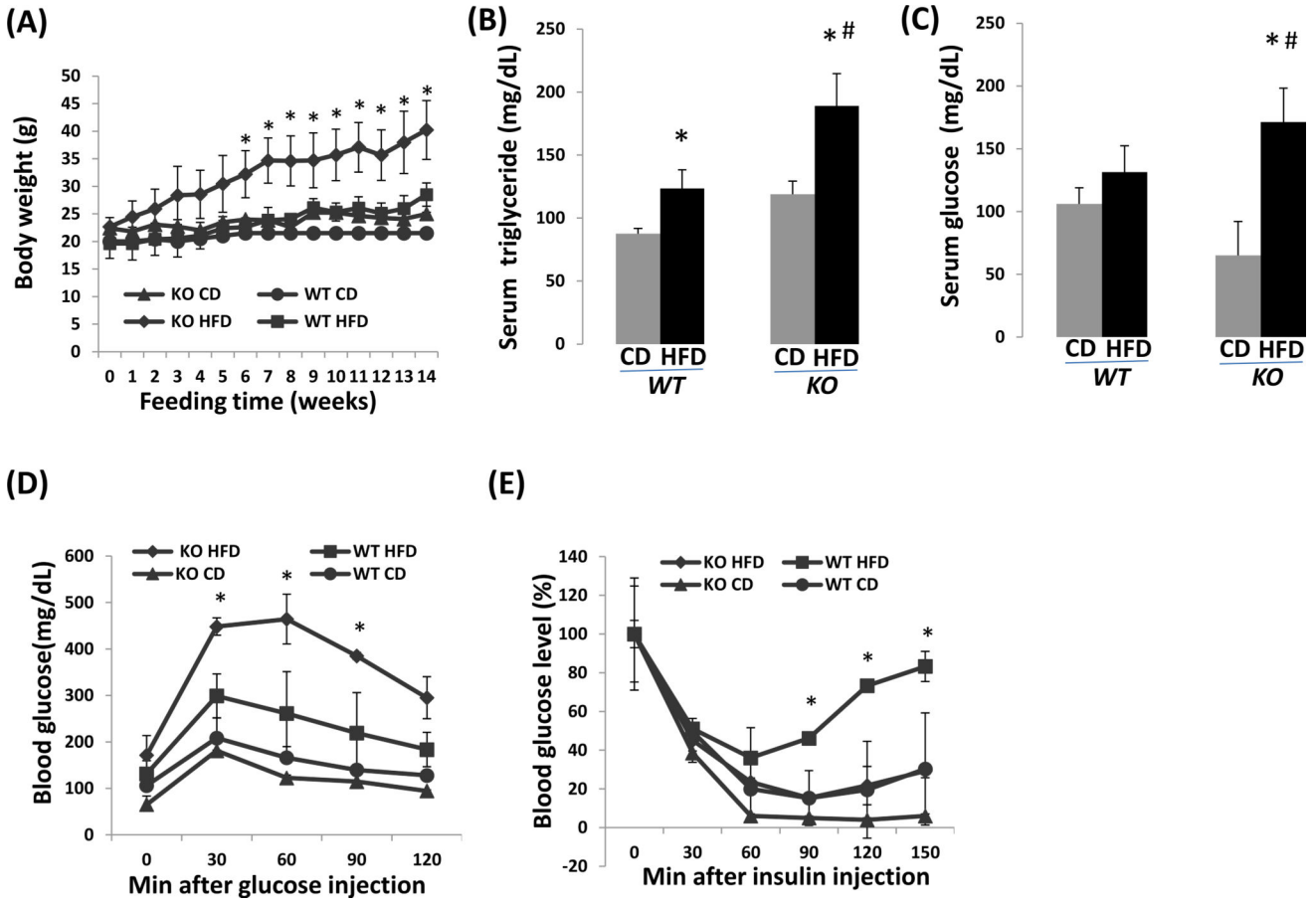

Figure 1.

HFD-induced obesity is more severe in cyp2a5$^{-/-}$ mice than in cyp2a5$^{+/+}$ mice. (A) Body weight. *P<0.05, compared with WT HFD group. (B) Serum triglyceride. *P<0.05, compared with CD group; #P<0.05, compared with WT HFD group. (C) Serum glucose. *P<0.05, compared with CD group; #P<0.05, compared with WT HFD group. (D) Glucose tolerance test. * P<0.05, compared with WT HFD group. (E) Insulin tolerance test. * P<0.05, compared with WT HFD group. CD, control diet; HFD, high fat diet; KO, cyp2a5$^{-/-}$ mice; WT, cyp2a5$^{+/+}$ mice.

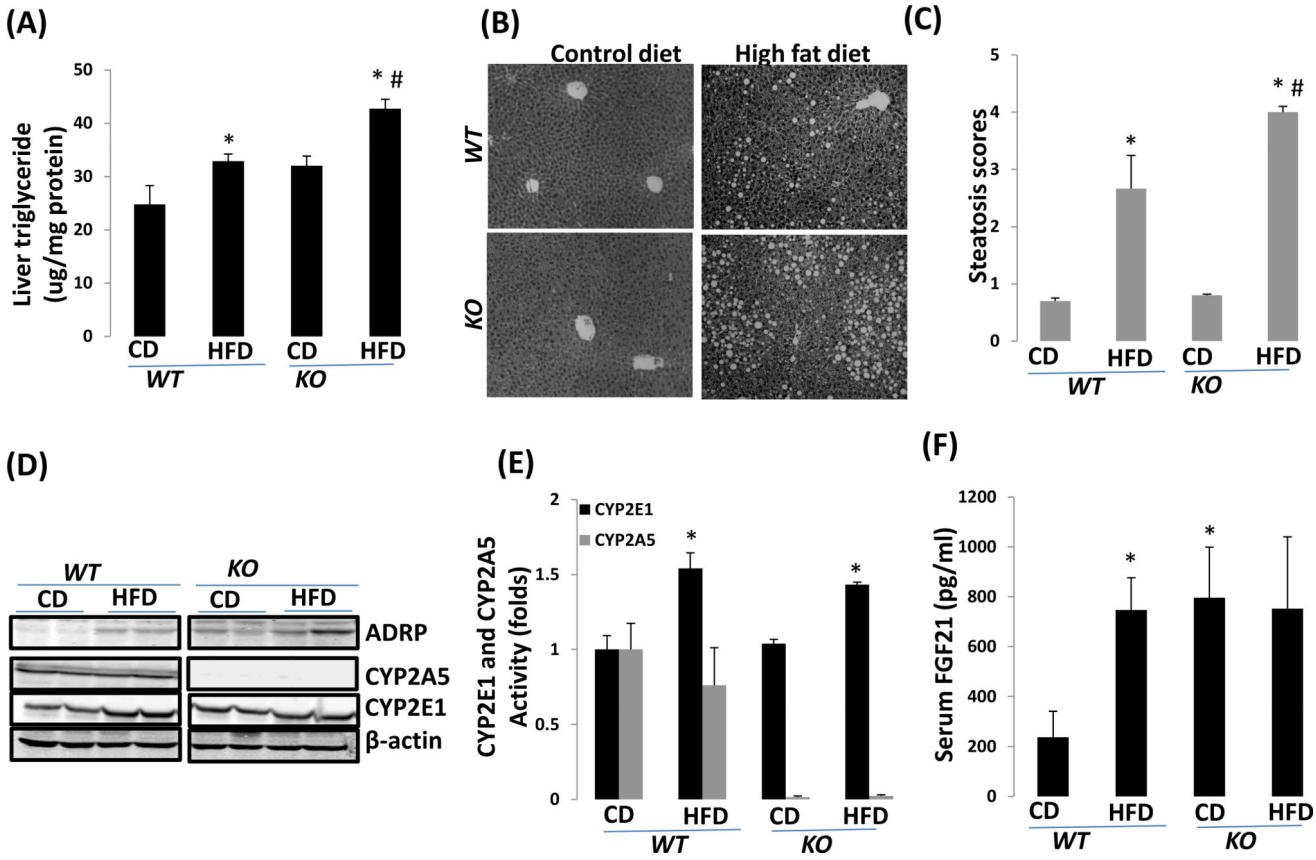

Figure 2.

HFD-induced nonalcoholic fatty liver is more severe in cyp2a5$^{-/-}$ mice than in cyp2a5$^{+/+}$ mice. (A) Liver triglyceride. *P<0.05, compared with CD group; #P<0.05, compared with WT HFD group. (B) Liver section H&E staining. (C) Pathological quantification: steatosis score. *P<0.05, compared with CD group; #P<0.05, compared with WT HFD group. (D) Liver expression of CYP2E1, CYP2A5, ADRP, PPARα and FGF21. (E) Activities of microsomal CYP2E1 and CYP2A5. *P<0.05, compared with CD group. (F) Serum FGF21 level. *P<0.05, compared with WT CD group.

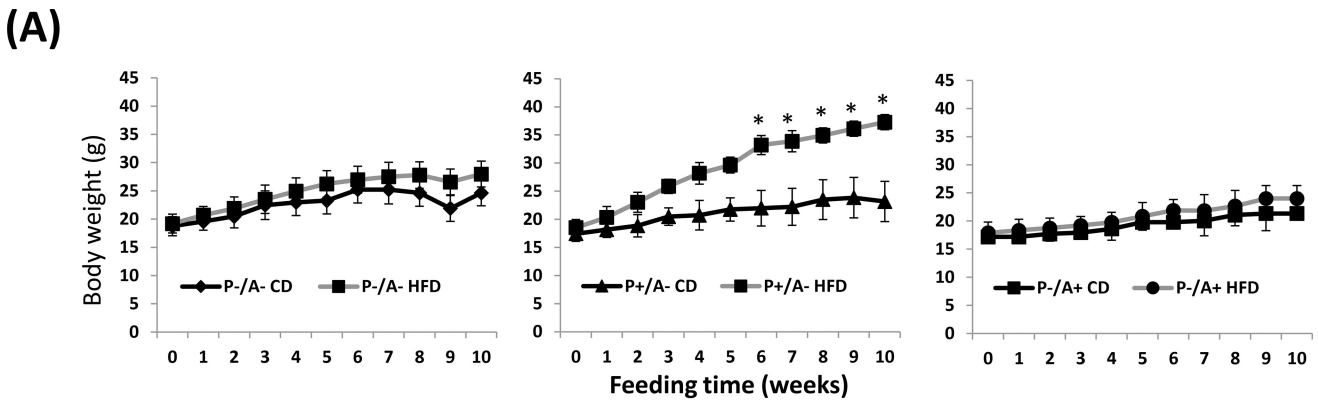

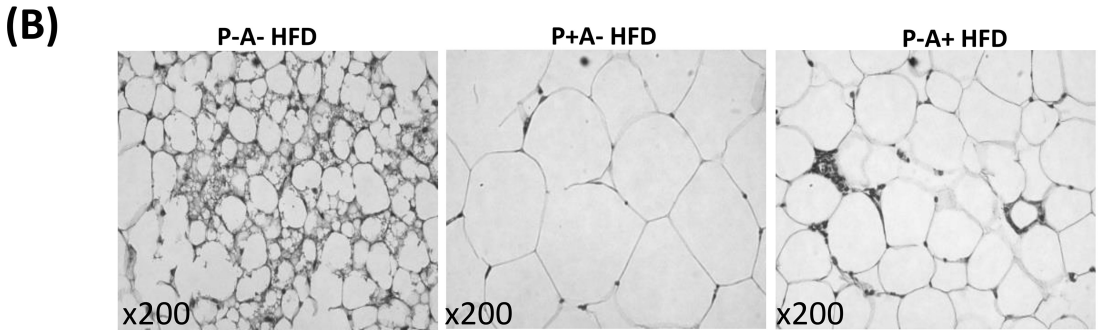

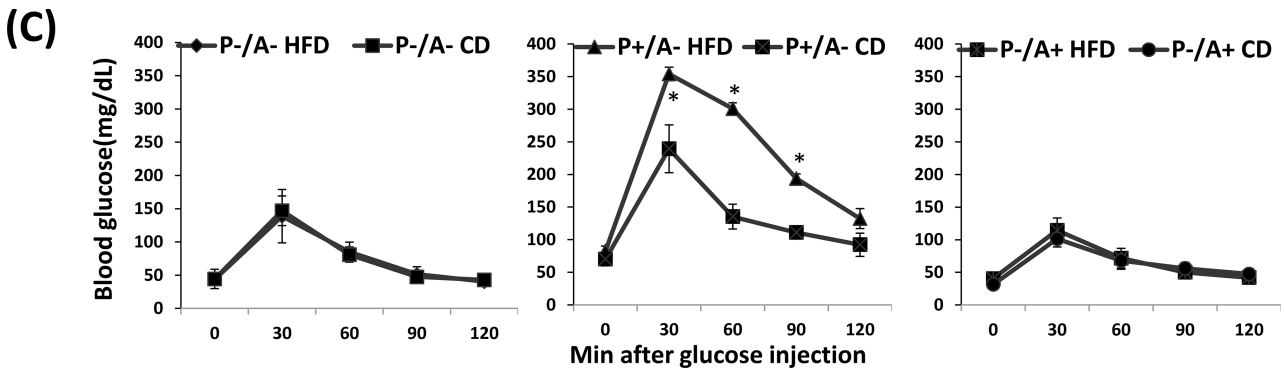

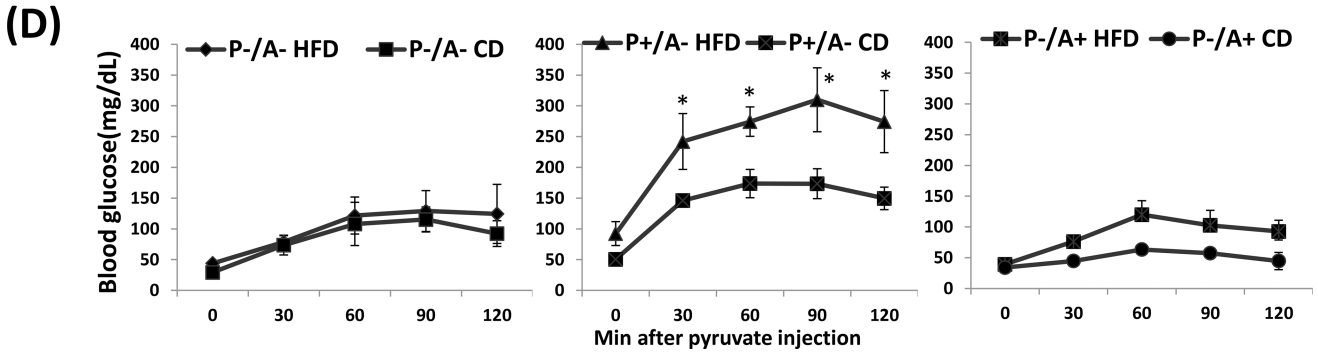

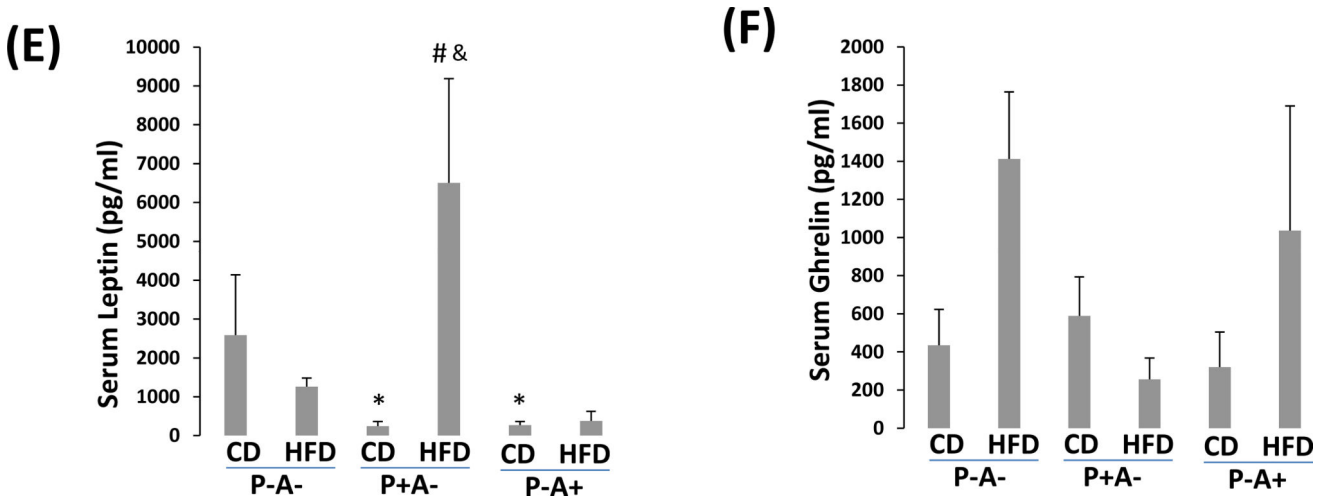

Figure 3.

HFD does not induce obesity in P-A- mice. (A) Body weight. (B). Adipose tissue H&E staining shows size of adipocytes. (C) Glucose tolerance test. (D) Pyruvate tolerance test. * $P<0.05$, compared to P+A- CD group. (E) Serum leptin. (F) Serum grhelin.

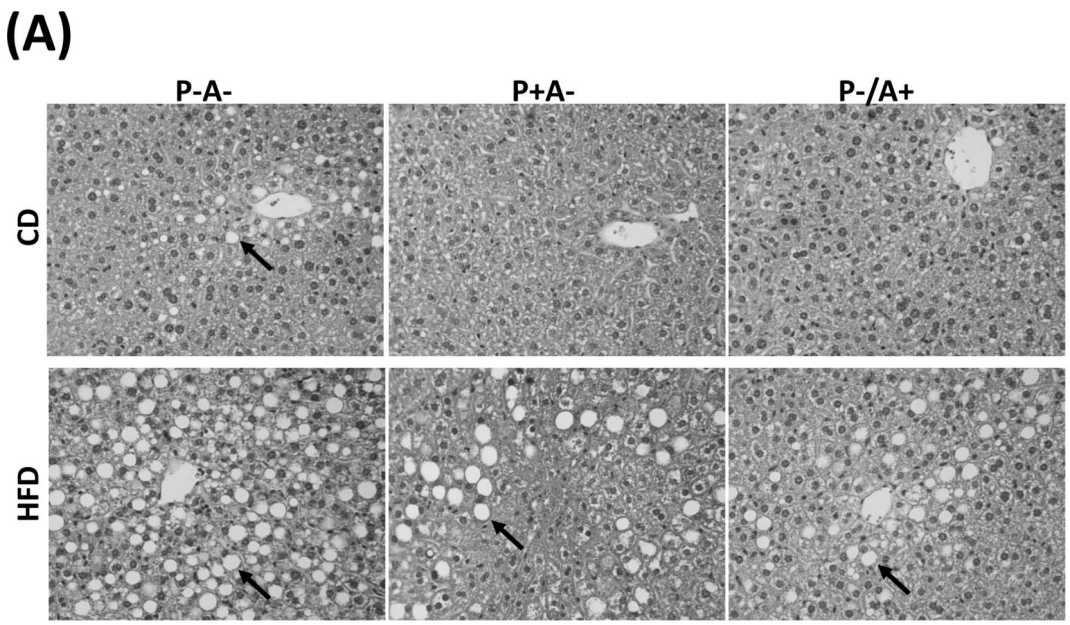

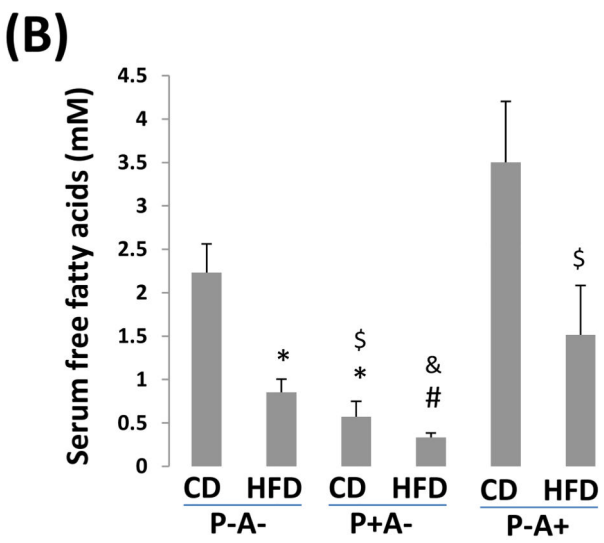

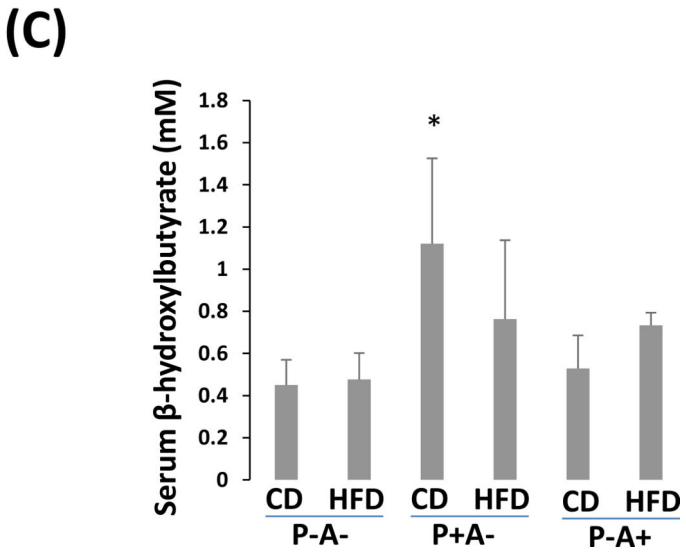

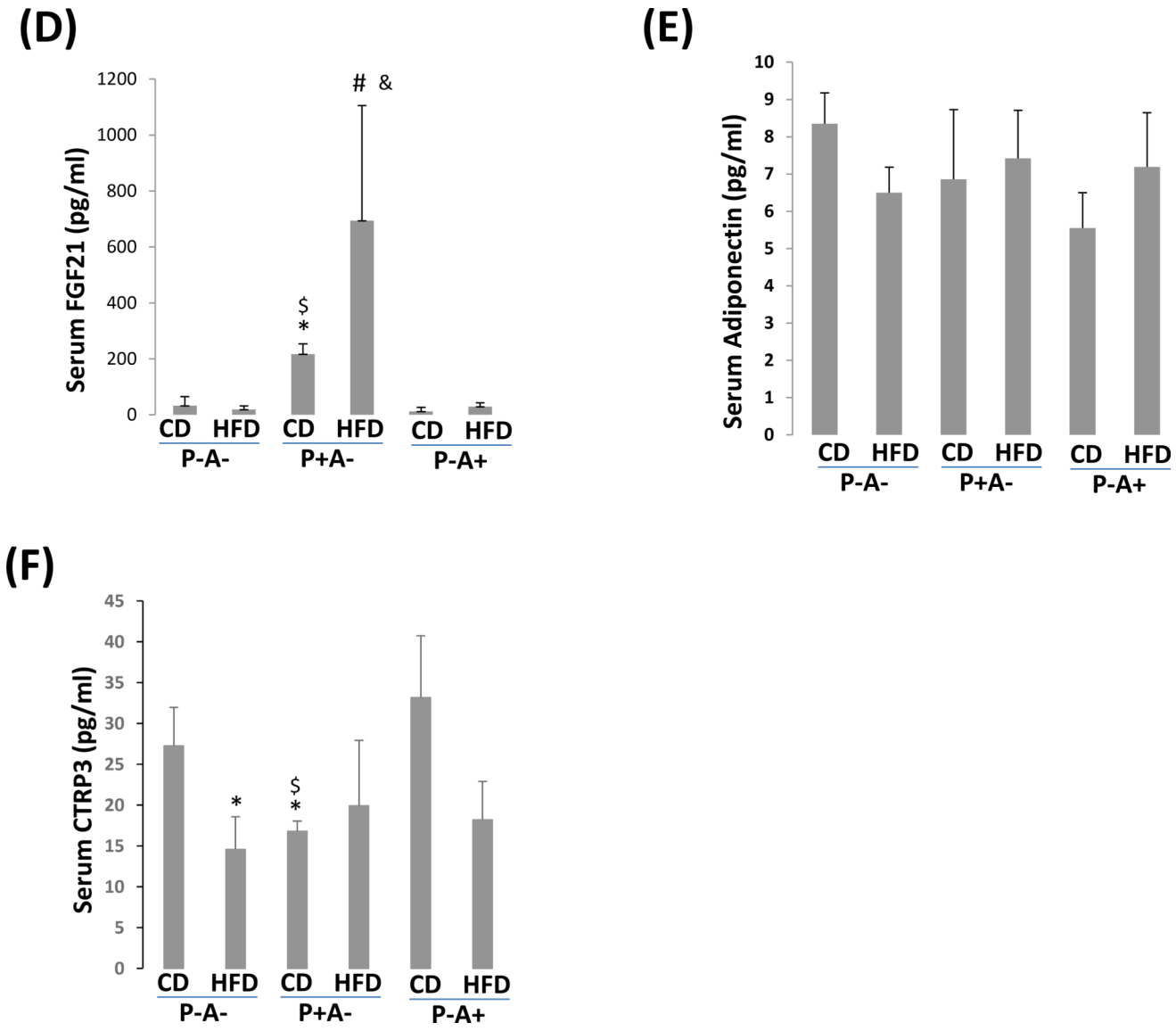

Figure 4.

HFD-induced fatty liver is more severe in P-A- mice than in P+A- mice. (A) Liver section H&E staining. Arrows show lipid droplets. (B) Serum levels of free fatty acids. (C) Serum β-hydroxylbutyrate. (D) Serum FGF21. (E) Serum adiponectin. (F) Serum CTRP3. *P<0.05, compared with P-A- CD group; $ P<0.05, compared with P-A+ CD group; # P<0.05, compared to P-A- HFD Group; & P<0.05, compared with P-A+ HFD group.

Int J Obes (Lond). Author manuscript; available in PMC 2020 March 01.

Table 1

Genetic association analysis of overweight and obesity

SNP	Position	Gene	A[a]	MAF[b]	HW[c]	OR-OB1[d]	p-OB1[e]	OR-OB2/3[f]	p-OB2/3[g]	OR-OW[h]	p-OW[i]
rs7251418	46033429	Cyp2f1p/Cyp2a6 *	A	0.26	0.805	0.79(0.57,1.10)	0.116	1.34(0.96,1.87)	0.0878	1.04(0.81,1.33)	0.759
rs8192729	46042836	Cyp2a6	A	0.09	0.999	1.94(1.21,3.10)	0.00582	0.94(0.49,1.8)	0.839	1.31(0.86,1.99)	0.208
rs4001921	46055141	Cyp2a6	G	0.26	0.761	0.79(0.57,1.09)	0.149	1.23(0.88,1.71)	0.218	0.96(0.75,1.23)	0.735
rs8102683	46055605	Cyp2a6	T	0.26	0.737	0.79(0.57,1.09)	0.149	1.23(0.88,1.71)	0.227	0.98(0.77,1.25)	0.86
rs8105704	46055738	Cyp2a6	T	0.26	0.847	0.79(0.58,1.10)	0.159	1.24(0.89,1.73)	0.203	0.97(0.76,1.24)	0.807
rs7256108	46056768	Cyp2a6	G	0.07	0.118	1.76(1.12,2.76)	0.0134	0.89(0.48,1.67)	0.72	1.26(0.85,1.88)	0.247
rs7255443	46056935	Cyp2a6	T	0.07	0.118	1.76(1.12,2.76)	0.0134	0.89(0.48,1.67)	0.72	1.26(0.85,1.88)	0.247
rs4453619	46076418	Cyp2a7 **	C	0.07	0.648	1.40(0.85,2.29)	0.183	0.92(0.48,1.75)	0.799	1.24(0.81,1.9)	0.322

[a] Minor allele;

[b] Minor allele frequency;

[c] p-value for Hardy-Weinberg equilibrium test;

[d] Odds ratio for obesity I based on logistic regression;

[e] p-value of obesity I based on logistic regression;

[f] Odds ratio for obesity II and III based on logistic regression;

[g] p-value of obesity II and III based on logistic regression;

[h] Odds ratio for overweight based on logistic regression;

[i] p-value of overweight based on logistic regression.

* Cyp2f1p

** Cyp2a7

Table 2

Haplotype analysis of class I obesity

SNPs	r^{2a}	Haplotype[b]	Frequency[c]	OR[d]	p[e]
rs8192729- rs7256108	0.94	A-G	0.08	1.94	0.00582
rs8192729-rs7256108	0.94	G-T	0.92	0.57	0.0134
rs8192729-rs7255443	0.94	A-T	0.08	1.94	0.00582
rs8192729-rs7255443	0.94	G-C	0.92	0.57	0.0134
rs8192729- rs4453619	0.73	A-G	0.02	3.83	0.00737
rs8192729- rs4453619	0.73	G-G	0.91	0.57	0.0143
rs7256108-rs7255443	1.00	G-T	0.08	1.76	0.0134
rs7256108-rs7255443	1.00	T-C	0.92	0.57	0.0134
rs7255443-rs4453619	0.75	T-G	0.02	3.0	0.0191
rs7255443-rs4453619	0.75	C-G	0.91	0.59	0.0184

[a] linkage disequilibrium measure (r^2);

[b] Haplotype inferred from 2 SNPs;

[c] Haplotype frequency;

[d] Odds ratio for each haplotype.

[e] *p*-value based on multiple logistic regression.